Reducing the metabolic energy of walking and running using an unpowered hip exoskeleton

Tiancheng Zhou
Huazhong University of Science and Technology - Main Campus: Huazhong University of Science and Technology
Caihua Xiong (chxiong@hust.edu.cn)
Huazhong University of Science and Technology https://orcid.org/0000-0003-2326-0289
Juanjuan Zhang
Nankai University
Di Hu
Huazhong University of Science and Technology - Main Campus: Huazhong University of Science and Technology
Wenbin Chen
Huazhong University of Science and Technology - Main Campus: Huazhong University of Science and Technology
Xiaolin Huang
Tongji Hospital of Tongji Medical College of Huazhong University of Science and Technology

Research

Keywords: Metabolic reduction, human walking and running, hip unpowered exoskeleton, hip flexion, human response

Posted Date: November 18th, 2020

DOI: https://doi.org/10.21203/rs.3.rs-107704/v1

Abstract

Background: Walking and running are the most common means of locomotion in human daily life. People have made advances in developing separate exoskeletons to reduce metabolic rate of walking or running. However, the combined requirements of overcoming fundamental biomechanical differences between the two gaits and minimizing the metabolic penalty of exoskeleton mass make it challenging to develop an exoskeleton that can reduce the metabolic energy for both gaits. Here we show that the metabolic energy of both walking and running can be reduced by regulating the metabolic energy of hip flexion during the common energy consumption period of the two gaits using an unpowered hip exoskeleton.

Methods: We analyzed metabolic rates, muscle activities and spatio-temporal parameters from 9 healthy subjects (mean s.t.d; 24.9 ± 3.7 years, 66.9 ± 8.7 kg, 1.76 ± 0.05 m) walking on a treadmill at the speed of 1.5 m×s -1 and running at speed of 2.5 m×s -1 with different spring stiffnesses. After obtaining the optimal spring stiffness, we recruited the participants to walk and run with the optimal stiffness spring at different speeds to demonstrate the generality of the proposed approach.

Results: We found that the optimal exoskeleton spring stiffnesses for walking and running were 140 N×m Rad -1 and 210 N×m Rad -1 respectively, corresponding to 8.2% ± 1.5% (mean ± s.e.m, two-sided paired t-test: $p < 0.01$) and 9.1% ± 1.3% ($p < 0.01$) metabolic reductions compared to walking/running without exoskeleton. The metabolic energy within tested speed range can be reduced with the assistance except for low speed walking (1.0 m s -1). Participants showed different changes in muscle activities with the assistance of proposed exoskeleton.

Conclusions: This paper first demonstrated that metabolic cost of walking and running can be reduced using an unpowered hip exoskeleton to regulate metabolic energy of hip flexion. The design method based on analyzing the common energy consumption characteristics between gaits may inspire future exoskeletons that assist multiple gaits. The results of different changes in muscle activities provided a new insight of human response to the same assistive principle in different gaits (walking and running).

Full Text

This preprint is available for download as a PDF.

Figures

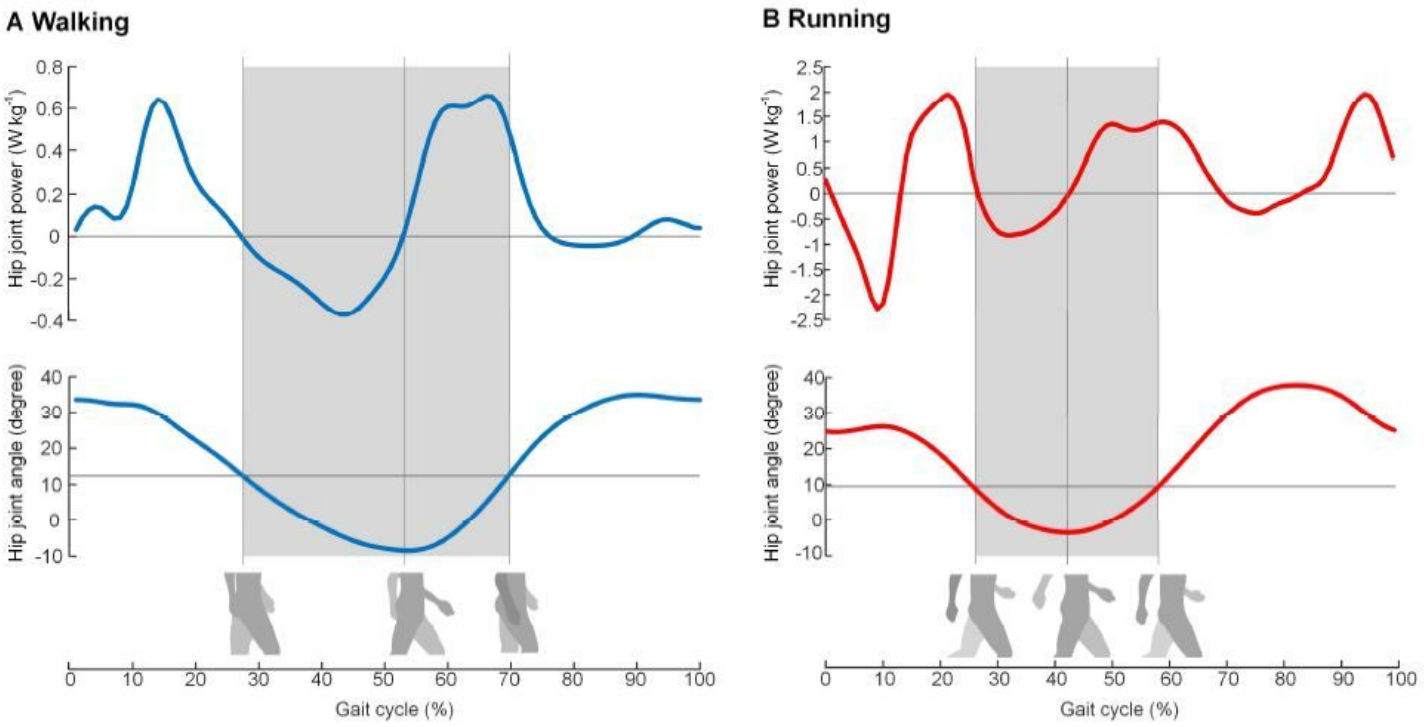

Figure 1

Hip joint power during walking and running. In the shaded interval of both walking and running, the hip joint extends from about 10 degrees of flexion position to the maximum extension position, corresponding to a period of negative power; Then, the hip joint flexes from the maximum extension position, corresponding to a period of positive work. The dataset of walking is the mean value of 7 participants (mean ± s.t.d; age, 26.9 ± 3.0 years; height,169.2 ± 7.0 cm; weight, 66.3 ± 14.2 kg), which is reported by [38]; The dataset of running is the mean value of 7 participants (mean ± s.t.d; age, 32.7 ± 5.6 years; height,176.9 ± 6.2 cm; weight, 67.0 ± 8.9 kg), which is reported by [39].

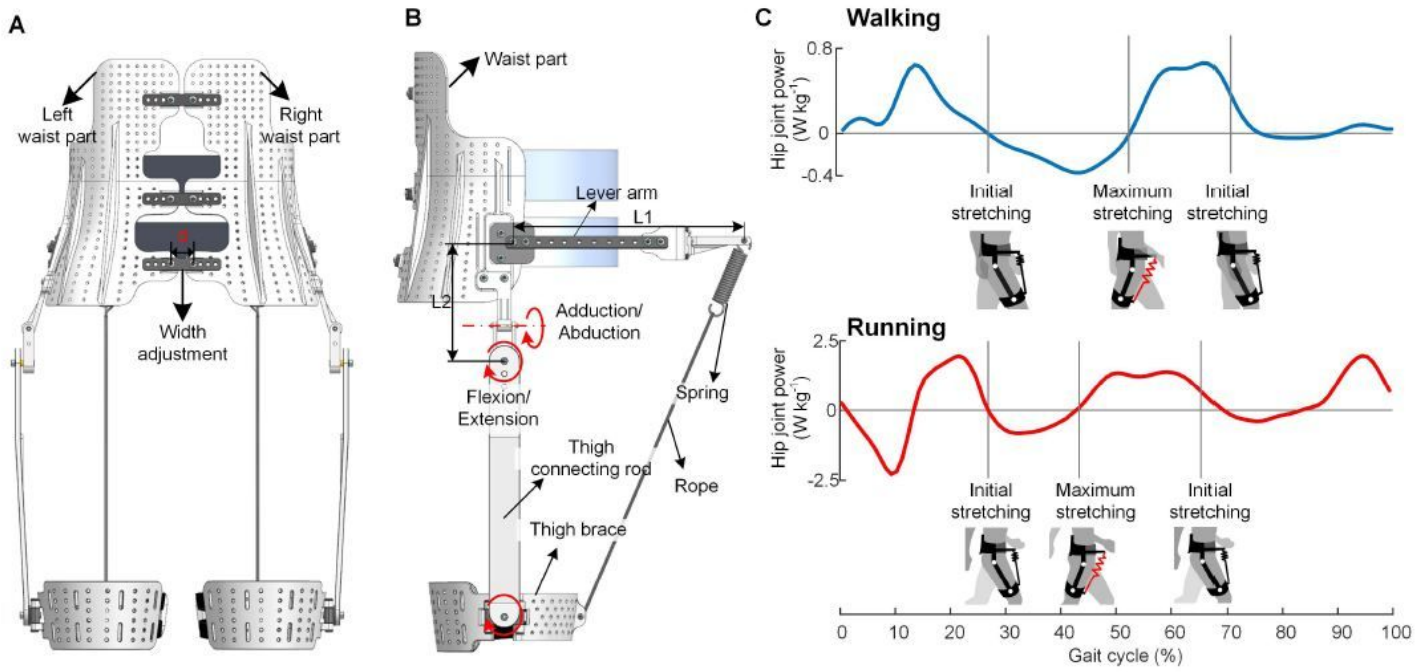

Figure 2

Exoskeleton components and working process of exoskeleton. (A) Back view of the exoskeleton. We change the length of d to adjust the width of the two waist parts for best fit participants. (B) Right view of the exoskeleton. The waist part and thigh connecting rods was connected using two rotary joints with plain bearing in series, allowing the adduction/abduction and flexion/extension of hip joint. (C) Working process of exoskeleton. The assistance interval is in accordance with the hip joint negative and positive mechanical power during walking and running. In the walking and running condition, the assistance started at nearly 10 degrees of hip flexion position. During the negative power period of the hip joint, the spring stores energy with the hip extension to its maximum extension position. During the positive power period of the hip joint, the spring releases the stored energy to assist hip flexion to 10 degrees of hip flexion position.

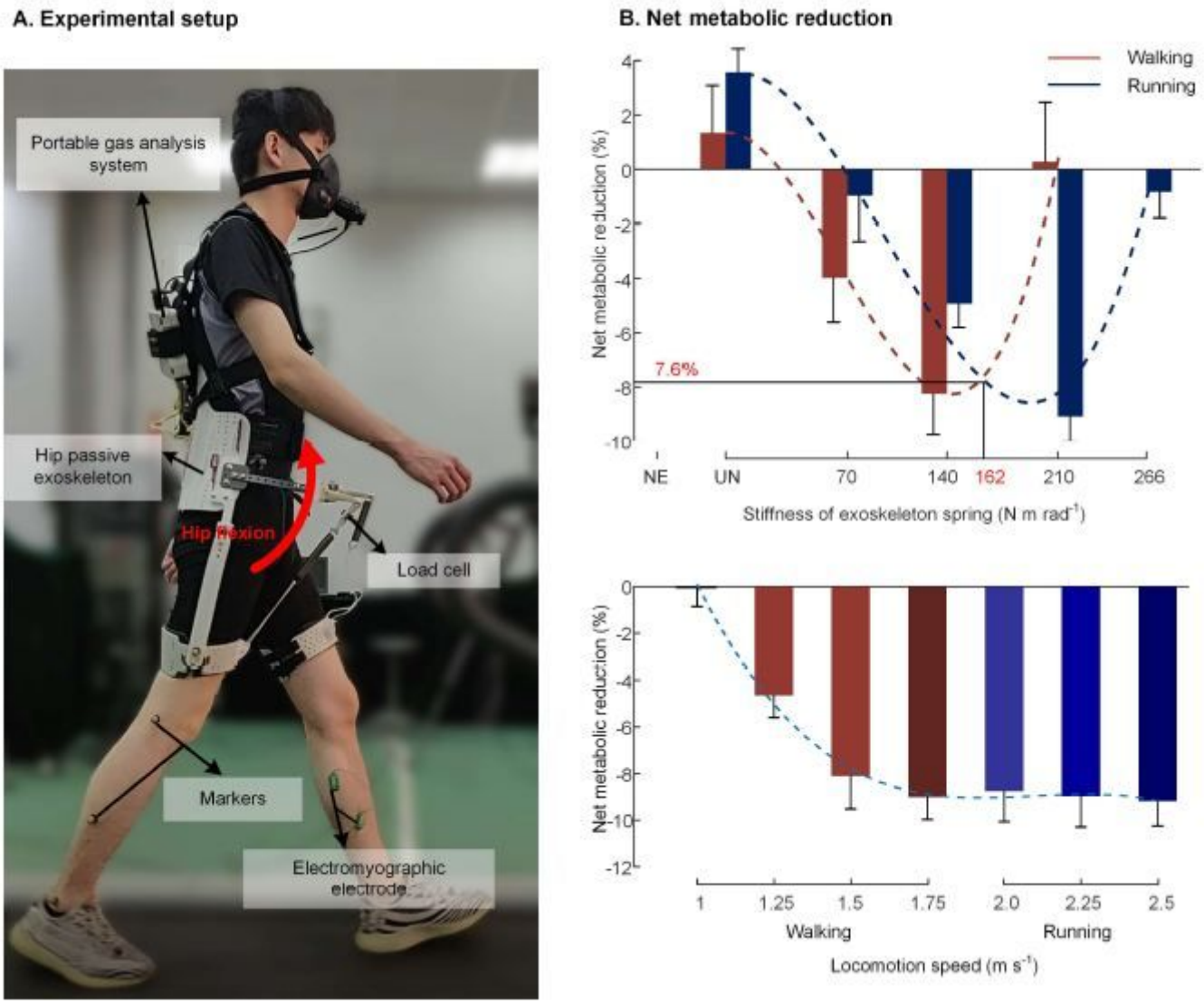

Figure 3

Experimental setup and metabolic reductions. (A) Experimental setup. While a participant was walking/running with the hip unpowered exoskeleton, the spring acted in front of the hip joint to provide hip flexion torque passively. The passive force of spring (load cell), lower limb segment motion (Vicon motion capture system), muscle activities (electromyography system) and metabolic rate (indirect calorimetry) were measured. (B) Net metabolic reduction. In the upper figure, Red color indicates walking conditions, and blue indicates running conditions. The red and blue dashed lines are the third-order best fit to mean metabolic reduction from stiffness conditions in walking and running (*p = 0.007; *p =0.037). The figure below shows the metabolic reduction during walking and running in different speeds. The blue dashed line is the third-order best fit to mean metabolic reduction from speed conditions in walking and running (R2 = 0.99, *p <0.001).

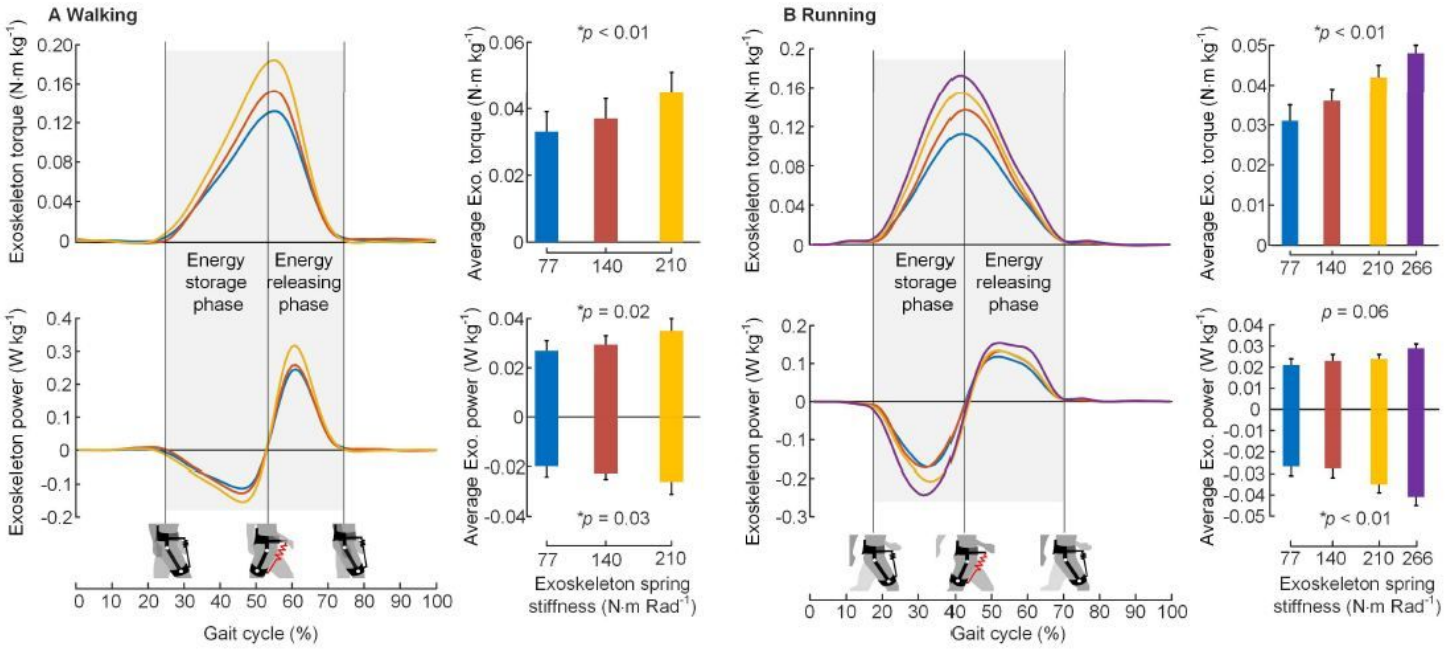

Figure 4

Exoskeleton torque and exoskeleton power. (A) and (B) The exoskeleton torque curve and power curve, which are normalized to body weight for each spring stiffness condition, averaged across participants during walking and running. The bar graphs on the right of the curves indicate the average exoskeleton torque, average exoskeleton positive and negative power. N = 9; error bars, s.e.m; p values are the results of mixed model two-way ANOVA (random effect: participant; fixed effect: spring stiffness).

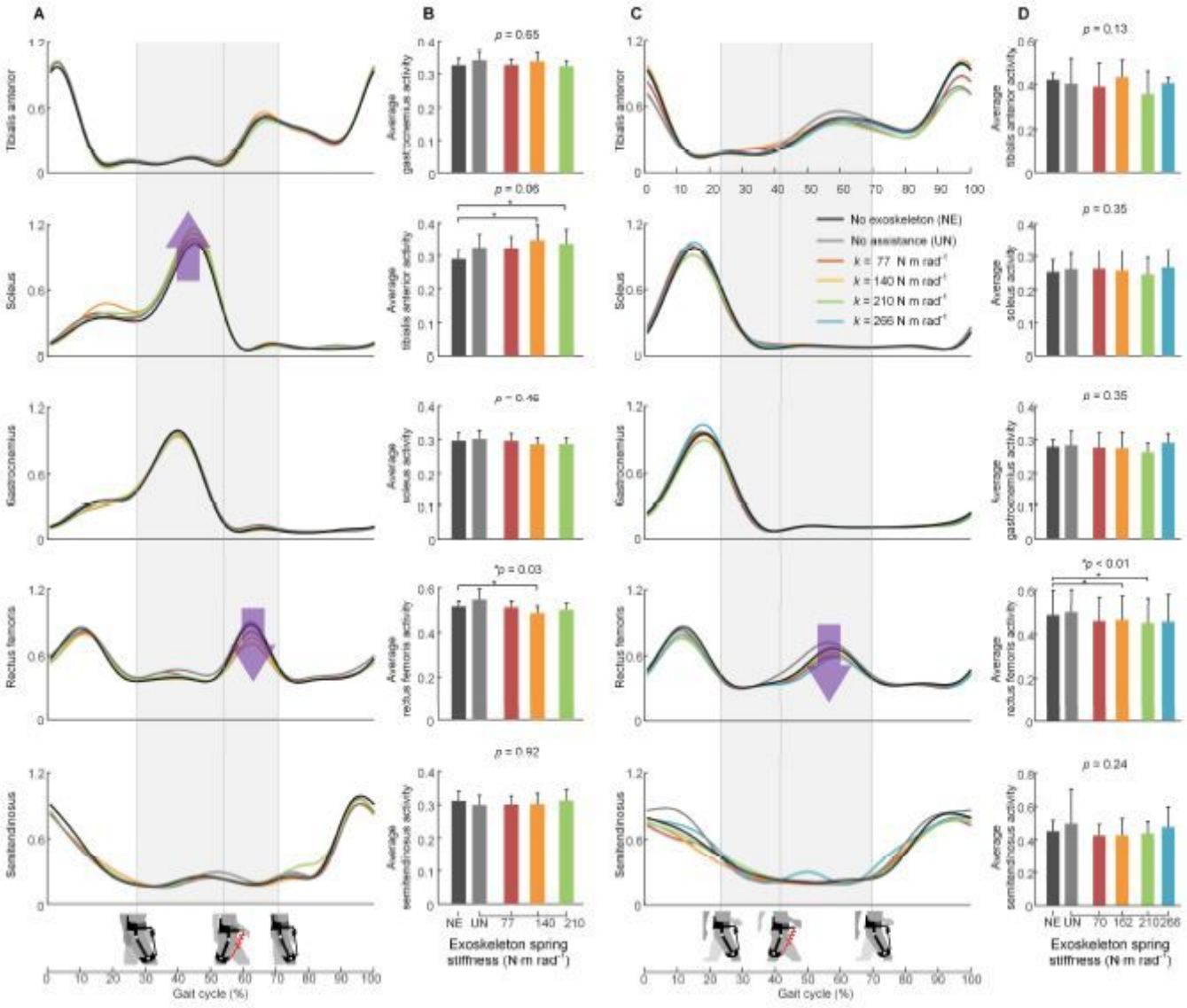

Figure 5

Changes in muscle activities during walking and running. (A) and (C) , activity of tibialis anterior (major ankle dorsiflexor), soleus (major ankle plantarflexor), gastrocnemius (major ankle plantarflexor), rectus femoris (major hip flexor) and semitendinosus (major ankle dorsiflexor) during walking and running. (B) and (D) columns, average muscle activity over the whole gait cycle for each condition. All values were measured using electromyography and normalized to maximum value in no exoskeleton condition (NE). N = 9; bars, mean; error bars, s.e.m; P values, mixed model two-way ANOVA (random effect: participant; fixed effect: spring stiffness). * indicates a significant difference compared to NE condition (two-sided paired t-test, $p < 0.05$).

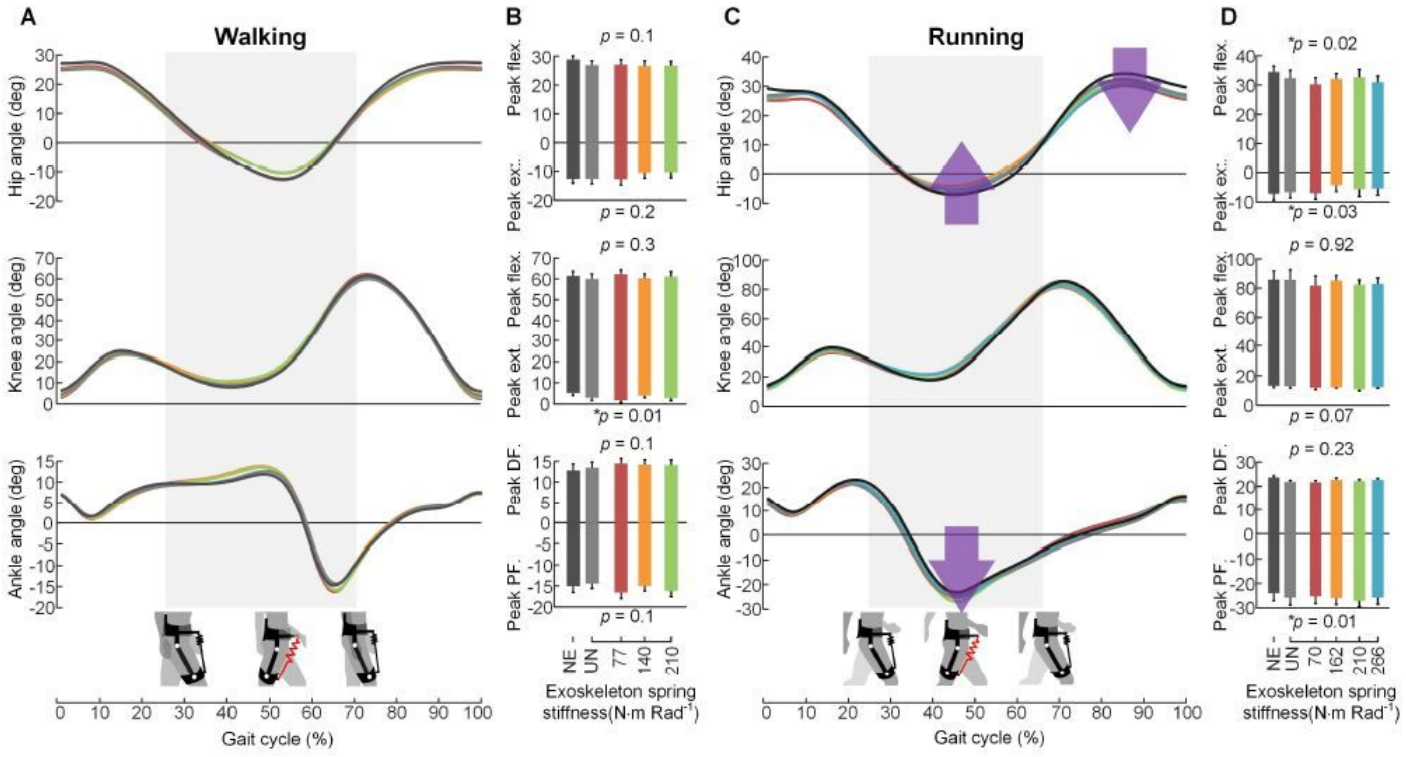

Figure 6

Changes in kinematics during walking and running. (A) and (C), The joint angles of hip, knee and ankle over the gait cycle, averaged by the 9 participants for each condition during walking and running. (B) and (D), The bar graphs are the peak flexion (flex.), extension (ext.), dorsiflexion (DF.) and plantarflexion (PF.) angles for each joint and each condition. N = 9; bars, mean; error bars, s.e.m; p values, mixed model two-way ANOVA (random effect: participant; fixed effect: spring stiffness).

Supplementary Files

This is a list of supplementary files associated with this preprint. Click to download.

- Additionalfile1.pdf